



Leaf nitrogen from first principles: field evidence for adaptive variation with climate

Ning Dong¹, Iain Colin Prentice^{1,2}, Bradley J. Evans^{1,3,4}, Stefan Caddy-Retalic^{5,6}, Andrew J. Lowe^{5,6,7}, Ian J. Wright¹

5 ¹Department of Biological Sciences, Macquarie University, North Ryde, NSW 2109, Australia

²AXA Chair of Biosphere and Climate Impacts, Department of Life Sciences, Imperial College London, Silwood Park Campus, Buckhurst Road, Ascot SL5 7PY, UK

³Terrestrial Ecosystem Research Network: Ecosystem Modelling and Scaling Infrastructure, University of Sydney, NSW 2006, Australia

10 ⁴Faculty of Agriculture and Environment, Department of Environmental Sciences, University of Sydney, NSW 2006, Australia

⁵Terrestrial Ecosystem Research Network: Australian Transect Network, University of Adelaide, North Terrace, Adelaide, SA 5005, Australia

15 ⁶School of Biological Sciences and Environment Institute, University of Adelaide, North Terrace, Adelaide, SA 5005, Australia

⁷Science, Monitoring and Knowledge Branch, Department of Environment, Water and Natural Resources, Hackney Road, Kent Town, SA 5005, Australia

Correspondence to: Ning Dong (ning.dong@mq.edu.au)



Abstract

Nitrogen content per unit leaf area (N_{area}) is a key variable in plant functional ecology and biogeochemistry. N_{area} comprises a structural component, which scales with leaf mass per area (LMA), and a metabolic component, which scales with Rubisco capacity. The co-ordination hypothesis, as implemented in LPJ and related global vegetation models, predicts that Rubisco capacity should be directly proportional to irradiance but should decrease with $c_i:c_a$ and temperature because the amount of Rubisco required to achieve a given assimilation rate declines with both. We tested these predictions using LMA, leaf $\delta^{13}C$ and leaf N measurements on complete species assemblages sampled at sites on a North-South transect from tropical to temperate Australia. Partial effects of mean canopy irradiance, mean annual temperature and $c_i:c_a$ (from $\delta^{13}C$) on N_{area} were all significant and their directions and magnitudes were in line with predictions. Over 80% of the variance in community-mean (\ln) N_{area} was accounted for by these predictors plus LMA. Moreover, N_{area} could be decomposed into two components, one proportional to LMA (slightly steeper in N-fixers), the other to predicted Rubisco activity. Trait gradient analysis revealed $c_i:c_a$ to be perfectly plastic, while species turnover contributed about half the variation in LMA and N_{area} .

Interest has surged in methods to predict continuous leaf-trait variation from environmental factors, in order to improve ecosystem models. Our results indicate that N_{area} has a useful degree of predictability, from a combination of LMA and $c_i:c_a$ – themselves in part environmentally determined – with Rubisco activity, as predicted from local growing conditions. This is consistent with a ‘plant-centred’ approach to modelling, emphasizing the adaptive regulation of traits. Models that account for biodiversity will also need to partition community-level trait variation into components due to phenotypic plasticity and/or genotypic differentiation within species, versus progressive species replacement, along environmental gradients. Our analysis suggests that variation in N_{area} is about evenly split between these two modes.

25

1 Introduction

Nitrogen (N) is an essential nutrient for primary production and plant growth, and nitrogen content per unit leaf area (N_{area}) is a key variable in plant functional ecology and biogeochemistry. A strong correlation between leaf N and photosynthetic capacity has been observed, and is to be expected



because typically almost half of the N in leaves is invested in the photosynthetic apparatus (Field and Mooney 1986; Evans and Seemann 1989; Evans 1989). This component of leaf N is approximately proportional to the maximum rate of carboxylation (V_{cmax}) at standard temperature (Wohlfahrt et al. 1999; Takashima et al. 2004; Kattge et al. 2009). Cell walls also account for a significant fraction of

5 leaf N (Lamport and Northcote 1960; Niinemets and Tenhunen 1997; Onoda et al. 2004). Leaf mass per area (LMA) is positively correlated with cell-wall N (Onoda et al. 2004) and is used as an index of plant investment in cell-wall biomass (Reich et al. 1991; Wright and Cannon 2001). Thus, to first order, N_{area} is the sum of a ‘metabolic’ component related to V_{cmax} and a ‘structural’ component proportional to LMA.

10 Dynamic Global Vegetation Models (DGVMs) are being extended to include interactive carbon (C) and N cycles (Thornton et al. 2007; Xu-Ri and Prentice 2008; Zaehle and Friend 2010). But there remain many open questions about the implementation of C-N coupling (Prentice and Cowling 2013), including the control of leaf N content, which is treated quite differently by different models. For example, any modelling approach that predicts photosynthetic capacity from N_{area} , and N_{area} in turn

15 from soil inorganic N supply (Luo et al. 2004), is incompatible with the hypothesis that photosynthetic capacity is optimized at the leaf level as a function of irradiance, leaf-internal CO₂ concentration (c_i) and temperature (Haxeltine and Prentice 1996, Dewar 1996) – as assumed in the widely used LPJ DGVM (Sitch et al. 2003) and other models derived from it, including LPJ-GUESS (Smith et al. 2001) and LPX (Prentice et al. 2011a; Stocker et al. 2013). This ‘plant-centred’ approach is based on the idea

20 that plant allocation processes determine leaf-level traits. More specifically it is derived from a long-standing concept, the ‘co-ordination hypothesis’, which states that the Rubisco- and electron transport-limited rates of photosynthesis tend to be co-limiting under average daytime conditions (Chen et al. 1993; Haxeltine and Prentice 1996; Maire et al. 2012). Co-limitation is optimal – even though mechanistically, it may be an inevitable outcome of leaf metabolism (Chen et al. 1993) – in the sense

25 that it provides the right balance of investments in the biochemical machineries for carboxylation and electron transport. It implies that enzyme activities adjust, over relatively long periods (weeks or longer), so that co-limitation holds. An important consequence is that the predicted responses of photosynthetic traits and rates to environmental variables observed in the field (whether temporally, comparing different seasons or spatially, comparing different environments) are substantially different from those

30 seen in short-term laboratory experiments. Specifically, V_{cmax} (and thus the metabolic component of



N_{area}) is predicted to be directly proportional to irradiance; to decrease with $c_i:c_a$; and to decrease with temperature. These predictions are supported in general terms by an observed positive relationship between N_{area} and irradiance (Field 1983; Wright et al. 2005), a negative relationship between N_{area} and $c_i:c_a$ (Wright et al. 2003; Prentice et al. 2011b; Prentice et al. 2014), and (in woody evergreens at least) a negative relationship between N_{area} and temperature (845 species: data from Wright et al. 2004). But there has been no systematic attempt to quantitatively assess the relationship of leaf N to environmental and structural predictors across environmental gradients. Such empirical work is needed to assess and underpin methods of C-N cycle coupling in DGVMs.

Here we set out to test the predictability of N_{area} using measurements carried out on dried plant material collected by the Terrestrial Ecosystem Research Network (TERN) AusPlots and Australian Transect Network facilities, at 27 sites on a north-south transect across the Australian continent. The transect extended from the wet-dry (monsoonal) tropics to the dry-wet (mediterranean) temperate zone via the arid interior, and encompassed substantial variation in all of the hypothesized controls of N_{area} (Fig. 1). The Ausplots protocol involves sampling all species within a 100×100 m plot (White *et al.* 2012). We measured N_{area} , $\delta^{13}C$ and LMA on all species at each site, and tested and quantified the effects of irradiance, $c_i:c_a$ ratio (from $\delta^{13}C$), temperature, LMA, and N-fixation ability (26% of the species sampled were N-fixers), on variation in N_{area} . The sampling design also allowed us to implement the trait gradient analysis method introduced by Ackerly and Cornwell (2007), which has been surprisingly little used to date. A growing body of field measurements shows extensive leaf-trait variation within species and PFTs (Kattge et al. 2011; Meng et al. 2015). Trait gradient analysis allows trait variation to be partitioned into a component due to variation within species and a component due to species replacement.

2 Materials and Methods

2.1 Climate data and analysis

Climatological data for the 27 sites were obtained from the eMAST/ANUclimate dataset (http://dapds00.nci.org.au/thredds/dodsC/rr9/Climate/eMAST/ANUclimate/0_01deg/v1m0_au/mon/land/catalog.html), which extends from 1970 to 2012 with 1 km spatial resolution across the entire continent. Mean annual precipitation (MAP) over this period at the sampling sites ranged from 154 to



1726 mm and mean annual temperature (MAT) from 14.1° to 27.6°C. The moisture index ($MI = P/E_q$, where P is mean annual precipitation and E_q is equilibrium evapotranspiration, calculated with the STASH program: Gallego-Sala et al. 2012) varied from 0.07 to 0.82. The mean incident flux of photosynthetically active radiation (PAR) during daylight hours, expressed as photosynthetic photon flux density ($\mu\text{mol m}^{-2} \text{s}^{-1}$), was also calculated using STASH. This incident flux (at the top of the canopy) was averaged through the canopy using Beer's law, as follows. First leaf area index (L) was estimated from remotely sensed (MODIS NBAR-derived using MOD43A4: <http://remote-sensing.nci.org.au/u39/public/html/modis/fractionalcover-clw>) fractional cover of photosynthetic vegetation (f_v) in 1 km resolution at each site, from data assembled by the TERN AusCover facility (Guerschman et al. 2009):

$$L \approx -(1/k) \ln(1 - f_v) \quad (1)$$

where $k = 0.5$. Then absorbed PAR per unit leaf area (I_L) was calculated as:

$$I_L \approx I_0 (1 - e^{-kL})/L \approx I_0 k f_v / \ln[1/(1 - f_v)] \quad (2)$$

where I_0 is the incident PAR above the canopy. This calculation yields $I_L \approx I_0$ for sparse vegetation ($L < 1$) but I_L becomes progressively smaller than I_0 as foliage density increases, reflecting the fact that the irradiance experienced by the average species is much lower in, say, a closed woodland than in an open shrubland, even if the PAR incident at the top of canopy is the same.

2.2 Foliage sampling and analysis

Mature sunlit leaves were sampled during the growing season using the AusPlots methodology (White et al. 2012). In total, the 27 selected sites included 442 unique species, of which 37 were C_4 plants (not analysed further here). LMA was measured on the archived leaf samples by scanning and weighing the leaves. Subsamples (a mixture of material from at least 2 replicates) were analysed for C and N contents and bulk $\delta^{13}\text{C}$ at the Stable Isotope Core Laboratory of Washington State University, USA. N_{area} was calculated from N content and LMA. Carbon isotope discrimination (Δ) values were derived from the reported $\delta^{13}\text{C}$ values using the standard formula:

$$\Delta = (\delta_{air} - \delta_{plant}) / (1 + \delta_{plant}) \quad (3)$$



where δ_{air} is the carbon isotope composition of air and δ_{plant} is the carbon isotope composition of the plant material. Because of the different diffusion rates and biochemical rates of carboxylation between $^{13}\text{CO}_2$ and $^{12}\text{CO}_2$, Δ can be used to estimate the $c_i:c_a$ ratio as:

$$c_i:c_a \approx (a + \Delta)/(b - a) \quad (4)$$

5 where the recommended standard values are $a = 4.4 \text{ ‰}$ and $b = 27 \text{ ‰}$ (e.g. Cernusak et al. 2013).

2.3 Analysis of V_{cmax}

Values of V_{cmax} were predicted based on the co-ordination hypothesis, by equating the carboxylation- and electron transport-limited rates of photosynthesis and, as a simplifying assumption, treating the electron transport-limited rate as proportional to absorbed PAR (i.e. ignoring the saturation of the
10 electron transport rate at high irradiances). These assumptions lead to the following estimate:

$$V_{cmax} \approx \varphi_0 I_L (c_i + K)/(c_i + 2\Gamma^*) \quad (5)$$

where φ_0 is the intrinsic quantum efficiency of photosynthesis (0.093; Long et al. 1993), c_i is the leaf-internal concentration of CO_2 , K is the effective Michaelis-Menten coefficient of Rubisco, and Γ^* is the photorespiratory compensation point. Both K and Γ^* were evaluated at standard atmospheric
15 pressure and oxygen concentration, and site MAT. Predicted values of V_{cmax} were adjusted to 25°C , because the amount of N allocated to Rubisco and other enzymes involved in carboxylation should be proportional to V_{cmax} at a standard temperature, not at the growth temperature. *In vivo* temperature dependencies of K , Γ^* and V_{cmax} were used for these calculations, following Bernacchi et al. (2001).

2.4 Statistic methods

20 All statistics were performed in R3.1.3 (R Core Team 2015). Linear regressions were fitted using the *lm* function, and partial residual plots generated using the *visreg* package. In a first, exploratory statistical analysis, a linear model was fitted for $\ln N_{area}$ with $c_i:c_a$, MAT, $\ln I_L$, $\ln \text{LMA}$ and the factor ‘N-fixer’ as predictors. The regression slopes of $\ln N_{area}$ against $c_i:c_a$, MAT and $\ln I_L$ can all be independently
25 predicted from the co-ordination hypothesis by differentiation of eq (5) (see Appendix A. Note that these formulae explicitly predict the slopes for $\ln N_{area}$). These predicted values were compared with the fitted values and their 95% confidence limits in order to assess support for the co-ordination hypothesis.



In a second analysis, community-mean values were calculated as simple averages across the species in each plot, omitting the factor ‘N-fixer’. A linear model was fitted to the community means of $\ln N_{area}$ as a function of $c_i:c_a$, MAT, $\ln I_L$ and $\ln LMA$ to assess the predictability of leaf N at the community level.

In a third analysis, N_{area} was modelled as a linear combination of the predictors Rubisco N, $N_{rubisco}$ (derived from predicted V_{cmax} at 25°C) and structural N, $N_{structure}$ (derived from LMA using the empirical relationship $N_{structure} = 10^{-2.67} LMA^{0.99}$, in $g\ m^{-2}$: Yusuke Onoda, personal communication 2015), including ‘N-fixer’ as a factor and allowing interactions of the predictors with this factor. An additional regression was performed with only $N_{structure}$ and $N_{rubisco}$ as predictors; their relative importance was calculated using the *relaimpo* package.

10 2.5 Trait gradients analysis

Trait gradients were generated for $\ln LMA$, $\ln N_{area}$ and $c_i:c_a$ following the analysis method of Ackerly and Cornwell (2007), again using simple averages across species to estimate community means. In this analysis species trait values were plotted against site-mean trait values. By definition, the regression of the species trait values against site-mean trait values has a slope of unity. For a perfectly plastic trait, regression of trait variation within species against the site-mean trait values would also yield a slope of unity. The common within-species slope that this approach provides is a measure of the fraction of trait variation due to phenotypic plasticity and/or genotypic variability. Its one-complement measures the fraction due to species turnover. Natural log transformation was applied to LMA and N_{area} because of their large variance and skewed distributions, but not to $c_i:c_a$ because of its small variance and approximately normal distribution.

3 Results

3.1 Leaf N variations with climate and leaf traits

Significant partial relationships were found for $\ln N_{area}$ versus $c_i:c_a$, MAT and $\ln I_L$ (Table 1, Fig. 2). The relationship was negative for $c_i:c_a$, as expected because lower $c_i:c_a$ implies that a greater photosynthetic capacity is required to achieve a given assimilation rate (or equivalently: a stronger CO₂ drawdown is enabled by a higher V_{cmax}). The relationship was also negative for MAT, as expected because there is an inverse relationship between temperature and the quantity of leaf proteins required



to support a given value of V_{cmax} . The relationship was positive for $\ln I_L$ (PAR), as expected because the higher the irradiance, the greater the carboxylation capacity required for co-limitation with the rate of electron transport.

Theoretical slopes for these relationships (derived in Appendix A) are compared with the fitted slopes in Table 1. For $\ln N_{area}$ versus $\ln I_L$, the theoretical slope is unity. The fitted slope of 0.874 (95% confidence limits: 0.685, 1.063) was statistically indistinguishable from unity. For $\ln N_{area}$ versus $c_i:c_a$, the fitted slope of -0.611 (-1.107 , -0.115) was fortuitously close to the theoretical slope of -0.615 , although the value was only weakly constrained for these data. For $\ln N_{area}$ versus MAT, the theoretical slope was obtained by subtracting the ‘kinetic’ slope of $\ln V_{cmax}$ versus temperature (from the activation energy of carboxylation as given by Bernacchi et al. 2001) from the shallow positive slope implied by eq (5). The kinetic effect was dominant, and results in an overall predicted negative slope of -0.048 . The fitted slope of -0.047 (-0.060 , -0.034) was indistinguishable from this theoretical slope, indicating acclimation to temperature by diminished allocation of N to metabolic functions at higher temperature, offsetting the increased reaction rate predicted by the Arrhenius equation. However this slope was shallower than would be predicted by the Arrhenius equation alone, reflecting the reduced quantum efficiency of assimilation (a higher V_{cmax} is required to support a given assimilation rate) at higher temperatures.

The proportion of leaf N allocated to Rubisco has generally been found to decline while the total N allocated to cell walls increases with increasing LMA (Hikosaka and Shigeno 2009). Fig. 2 shows a strong positive partial relationship between $\ln N_{area}$ and LMA. N-fixers had generally higher N_{area} than non-N-fixers (Fig. 2e: $p < 0.001$). The predictors together explained 55% of the variation in leaf N across species and sites.

Fully 82% of the variation in the community-mean value of $\ln N_{area}$ could be explained by the combination of community-mean LMA and environmental variables. Significant partial relationships of community-mean $\ln N_{area}$ with MAT, $\ln I_L$ and $\ln LMA$ (Table 2) were consistent with the results obtained at species level. The fitted slopes of $\ln N_{area}$ against $\ln I_L$ and MAT were again indistinguishable from the theoretical values, albeit with wide error bounds due to the much smaller sample size (27 as opposed to 405). The community-level partial relationship between $\ln N_{area}$ and $c_i:c_a$ showed a negative slope as predicted, but this relationship was non-significant ($p \approx 0.1$).



3.2 Leaf N as the sum of metabolic and structural components

Highly significant ($p < 0.001$) positive relationships were found between N_{area} and the predicted Rubisco-N content per unit leaf area ($N_{rubisco}$), and the predicted cell wall N content per unit leaf area ($N_{structure}$) (Fig. 3). *A priori* we would expect the regression coefficient for $N_{structure}$ to be close to unity, and that for $N_{rubisco}$ to be about 6 to 20 (if Rubisco constitutes about 5 to 15% of total leaf protein: Evans 1989; Evans and Seemann 1989; Onoda et al. 2004). The fitted slopes of 1.2 ($p < 0.001$; 95% confidence limits: 1.0, 1.4) and 9.5 ($p < 0.001$; 7.6, 11.5) in Table 3, respectively, were consistent with these expectations.

There was no significant main effect of the factor ‘N-fixer’, and no significant interaction between $N_{rubisco}$ and the factor ‘N-fixer’. The co-ordination hypothesis predicts that the metabolic component of N_{area} should be environmentally optimized, and therefore independent of N supply. This could not be tested without measurements of V_{cmax} or $N_{rubisco}$, which were precluded by the design of this study. However, N-fixers showed a steeper relationship between N_{area} and $N_{structure}$. This was manifested as a significant interaction between the factor ‘N-fixer’ and $N_{structure}$ ($p < 0.01$). This model, in which N_{area} was decomposed into a metabolic component predicted by the co-ordination hypothesis and a structural component proportional to LMA, explained 52% of the variance in N_{area} across species and sites. The relative importance of variations in the metabolic and structural components, were determined to be 39% and 61% respectively (in an analysis with only $N_{rubisco}$ and $N_{structure}$ as predictors), showing *inter alia* the importance of variation in LMA in determining leaf N content.

3.3 Quantifying trait plasticity versus species turnover

In total, 243 C_3 species were sampled at two or more sites. These species allowed calculation of a common slope, being an estimate of trait plasticity *sensu lato* (that is, phenotypic plasticity or genetic adaptation or both) across species (Fig. 4), for the traits $c_i:c_a$, \ln LMA and \ln N_{area} . Contrasting results were obtained for the three traits. It appeared that $c_i:c_a$ is perfectly plastic, with a common (within-species) slope indistinguishable from unity. The slope of N_{area} was close to 0.5, indicating approximately equal contributions of plasticity and species turnover to the total variation. In the case of LMA, however, there was significant heterogeneity ($p < 0.05$) among the within-species slopes, with *Marsdenia viridiflora* showing a significantly steeper slope than the other species. After excluding this



species, the common slope for LMA was also close to 0.5. A positive common slope indicates the ability of species to adapt their leaf morphology to environment. The positive common slope found for N_{area} is consistent with this trait's nature as a combination of metabolic and structural components; its similarity to the slope for LMA is consistent with the importance of variations in structural N in
5 determining total N.

4 Discussion

4.1 Leaf N and environment

The variety of environments provided in this study by the long transcontinental transect, and the number of species sampled, allowed us to statistically separate the effects of $c_i:c_a$, irradiance, temperature and
10 LMA on N_{area} . The relationships to $c_i:c_a$, irradiance and temperature were in the directions and general magnitudes predicted by the co-ordination hypothesis.

High N_{area} in plants from arid environments has been described often, and has traditionally been explained as a consequence of high N supply in environments with low rainfall (reducing leaching losses) and restricted plant cover (reducing total vegetation N demand) (e.g. Field and Mooney 1986).
15 This explanation would imply that plants in wetter environments have lower (and suboptimal) N_{area} due to low *availability* of N. However, the negative relationship commonly found between $c_i:c_a$ and N_{area} supports an alternative, adaptive explanation. The least-cost hypothesis (Wright et al. 2003; Prentice et al. 2014) predicts lower $c_i:c_a$ in drier environments, due to the increased water transport capacity needed to support a given rate of assimilation in a drier atmosphere. When $c_i:c_a$ is lower, the co-ordination
20 hypothesis predicts that a higher V_{cmax} (and therefore higher N_{area}) is optimal, in order for the leaves to fully utilize the available light. The co-ordination hypothesis also predicts a further increase in N_{area} with increasing aridity due to reduced cloudiness and reduced shading by competitors, both factors tending to increase I_L . Thus the co-ordination hypothesis could account for independent positive effects of site irradiance and aridity on N_{area} , as previously reported by Wright et al. (2005). The fitted
25 relationship of N_{area} to temperature, PAR and $c_i:c_a$ is consistent with our theoretical prediction, which implicitly includes all of these effects.

Despite the large within-site variation in LMA found at all points along the aridity gradient, there is a significant tendency for LMA to increase with aridity, perhaps because of the resistance to dehydration



conferred by stiffer leaves (Niinemets 2001; Wright and Westoby 2002; Harrison et al. 2010), and/or the need for leaves to avoid overheating under transient conditions of high radiation load and low transpiration rates combined with low wind speed (Leigh et al. 2012). This increase in LMA is inevitably accompanied by an increasing structural N component.

- 5 Thus, several distinct aspects of plant allocation tend to increase N_{area} along gradients of increasing dryness. The predicted response of $N_{rubisco}$ to temperature is a result of opposing effects: the declining efficiency of photosynthesis with increasing temperature (due to the temperature dependencies of K and Γ^*) is offset by the increased catalytic capacity of Rubisco at higher temperatures. The latter effect is predicted to be stronger, implying reduced N_{area} with increasing temperature, as observed.

10 4.2 The predictability of leaf N

Predicted $N_{rubisco}$ and $N_{structure}$ together explained more than half of the variation in total N_{area} across species and sites. Our approach to predicting these two quantities invokes a simplified formula, eq (5), which is based on the co-ordination hypothesis for $N_{rubisco}$, assuming proportionality with Rubisco capacity; and assumes a simple proportionality with LMA for $N_{structure}$. In reality, leaf N includes other
15 photosynthetic proteins, including proteins of the light-harvesting complexes and electron transport chains, cytosolic proteins, ribosomes and mitochondria, nucleic acids (which account for about 10–15% of leaf N: Chapin III and Kedrowski 1983), and N-based defensive compounds. It is possible that the higher N found for N-fixers resides in N-based osmolytes (Erskine et al. 1996) or defence compounds (Gutschick 1981). Nonetheless, our simplifications suggest that N_{area} – especially at the community
20 level, which is key for large-scale modelling – is, to first order, inherently predictable from leaf morphology and the physical environment. A corollary is that limitation in N supply may act primarily by changing plant allocation patterns (reducing allocation to light capture by leaves, while increasing allocation to N uptake by roots), rather than by altering leaf stoichiometry.

4.3 Trait variations within and between species

- 25 By testing for acclimation along spatial gradients, the design of our study did not allow phenotypic plasticity to be distinguished from genetic adaptation. Phenotypic plasticity is the ability of a genotype to alter its expressed trait values in response to environmental conditions (Bradshaw 1965; Sultan 2000). A part of the observed variation in trait values within species could be due to shifts in the occurrence



and frequency of different genotypes, producing different preferred trait values. Thus, when we refer to traits as ‘plastic’ this should be understood in a broad sense to allow the possibility of a genetic component of the observed adaptive differentiation within species. Seasonal acclimation within individual plants can provide more direct evidence for phenotypic plasticity (Togashi *et al.*, in revision),
5 whereas in this study we disregard possible seasonal variations and instead relate trait variations to the mean annual environment. However, by sampling all of the species present at each site and including measurements on species at multiple sites, we could distinguish between the contribution of plasticity *sensu lato* (phenotypic plasticity and/or genetic adaptation) versus species turnover, i.e. the progressive replacement of species with different mean trait values, to spatial variation in the community mean
10 values of a given trait. We found that $\delta^{13}\text{C}$ was perfectly plastic, perhaps not surprisingly as variations in $c_i:c_a$ are under stomatal control. In contrast, LMA and N_{area} showed approximately equal contributions from plasticity and species turnover.

4.4 Implications for modelling

There has been a surge of interest in schemes to predict continuous trait variation in DGVMs (e.g.
15 Scheiter *et al.* 2013; Fyllas *et al.* 2014; van Bodegom *et al.*, 2014; Ali *et al.* 2015; Fisher *et al.* 2015; Meng *et al.* 2015; Sakschewski *et al.* 2015). Some trait-based modelling approaches have relied on empirical information on trait-trait and trait-environment covariation, but others (e.g. Scheiter *et al.* 2013) have aimed to represent the adaptive nature of trait variation explicitly. Our focus has been on testing an explicit adaptive hypothesis for the controls of one key trait, N_{area} , which in addition to a
20 structural component (necessarily linked to LMA) includes an important metabolic component, reflecting the leaf-level investment in photosynthetic proteins. We have shown that N_{area} is predictable to a degree that is useful for modelling. Our prediction is based on LMA, $c_i:c_a$ and a predicted value of V_{cmax} based on the co-ordination hypothesis, for which there is strong independent evidence (e.g. Maire *et al.* 2012). The partial responses of N_{area} to $c_i:c_a$, irradiance and temperature are consistent with
25 predictions of the co-ordination hypothesis, and the inclusion of predicted V_{cmax} adds significantly and substantially to the predictive power of LMA and $c_i:c_a$ alone. As both LMA (Wright *et al.* 2005) and $c_i:c_a$ (Prentice *et al.* 2014) show relationships to environment, our results suggest a possible route towards a general adaptive scheme for the prediction of major leaf traits in DGVMs. They also suggest



some priorities for trait data collection and analysis: to test the predicted controls of N_{area} over a wider range of environments, and to test the predicted environmental controls of V_{cmax} directly in the field.

Our application of trait gradient analysis also points out a way towards process-based treatments of functional trait diversity in next-generation models. It is increasingly accepted that models could, and should, sample ‘species’ from continuous gradients of traits rather than fixing the traits associated with discrete PFTs. A hybrid approach to modelling N_{area} based on the present analysis would consider N_{area} explicitly as the sum of metabolic and structural components. The metabolic component would be treated as plastic, and subject to environmental optimization (in space and time) consistent with the least-cost and co-ordination hypotheses. The structural component would be tied to LMA, which is a key variable of the ‘leaf economics spectrum’ (Wright et al. 2004), strongly expressed both within and between environments and therefore requiring a broad range of values to be assigned to model ‘species’.

Finally, we note that if our results can be corroborated more widely, this would point to the need for a shift in the way N ‘limitation’ is treated – both in models and in analyses of field data. In studies of the relationship between V_{cmax} and leaf N, for example, it is conventional to plot N on the x-axis and V_{cmax} on the y-axis, and it is then often stated that the positive relationship found shows that variation in leaf N ‘causes’ variation in V_{cmax} . But all that is shown on the graph is a correlation, and our ‘plant-centred’ interpretation is the opposite of the conventional one: that is, V_{cmax} is adaptively matched (acclimated) to environmental conditions, and the metabolic component of leaf N is a consequence of this acclimation. Low N availability would then result in reduced allocation of C (and N) to leaves, and increased allocation below ground – which is also an adaptive response, but at the whole-plant rather than the leaf level.



Appendices

Appendix A: Theoretical responses of N_{area} to environmental predictors

We estimate optimal V_{cmax} by $\varphi_0 I_L (c_i + K)/(c_i + 2\Gamma^*)$ (eq 5). Holding other variables constant, the sensitivity of this estimate to absorbed PAR is given by the derivative of its natural logarithm with respect to $\ln I_L$:

$$\partial \ln V_{cmax} / \partial \ln I_L = 1 \quad (\text{A1})$$

Similarly, the sensitivity of this estimate to c_i is given by:

$$\partial \ln V_{cmax} / \partial c_i = (2\Gamma^* - K) / [(c_i + K)(c_i + 2\Gamma^*)] \quad (\text{A2})$$

and its sensitivity to the $c_i:c_a$ ratio is smaller than this by a factor c_a .

10 Temperature-dependent reaction rates are described by the Arrhenius equation:

$$\ln x(T) - \ln x(T_{ref}) = (\Delta H/R) (1/T_{ref} - 1/T) \quad (\text{A3})$$

where x is the rate parameter of interest, T is the measurement temperature (K), T_{ref} is the reference temperature (here 298 K), ΔH is the activation energy of the reaction ($\text{J mol}^{-1} \text{K}^{-1}$) and R is the universal gas constant ($8.314 \text{ J mol}^{-1} \text{K}^{-1}$). Linearizing eq (A3) around T_{ref} yields:

$$15 \quad \ln x(T) - \ln x(T_{ref}) \approx (\Delta H/RT_{ref}^2) \Delta T \quad (\text{A4})$$

where $\Delta T = T - T_{ref}$. Thus, from equation (5):

$$\ln V_{cmax25} \approx \ln V_{cmax} - (\Delta H_v/RT_{ref}^2) \Delta T \quad (\text{A5})$$

where ΔH_v is the activation energy of V_{cmax} . The sensitivity of V_{cmax25} to T is then:

$$20 \quad \begin{aligned} \partial \ln V_{cmax25} / \partial T &= \partial \ln V_{cmax} / \partial T - (\Delta H_v/RT_{ref}^2) \\ &= (\partial K / \partial T) / (c_i + K) - 2(\partial \Gamma^* / \partial T) / (c_i + 2\Gamma^*) - (\Delta H_v/R/T_{ref}^2) \end{aligned} \quad (\text{A6})$$

where $K = K_c(1 + O/K_o)$, hence:

$$\partial K / \partial T = \partial K_c / \partial T + [(\partial K_c / \partial T) K_o - (\partial K_o / \partial T) K_c] O / K_o^2 \quad (\text{A7})$$



where O is the atmospheric concentration of oxygen and Γ^* and the Michaelis-Menten coefficients for carboxylation (K_C) and oxygenation (K_O) respectively have values at T_{ref} (in $\mu\text{mol mol}^{-1}$) and activation energies as given by Bernacchi *et al.* (2001).

Author contribution

5 ICP, ND and AJL planed and designed the study; ND carried out all the field measurement and performed the data analyses. ND and ICP wrote the first draft; BJE supported the study through provision of climate data; IJW assisted with data interpretation, contributed with ideas throughout and suggested important improvements to the text. SCR contributed important ideas to improve text. All authors contributed on subsequent versions.

10 Acknowledgments

Research funded by the Terrestrial Ecosystem Research Network (TERN) through the AusPlots, Australian Transect Network and eMAST facilities. DN is supported by an international Macquarie University Research Scholarship. IJW has been supported by an Australian Research Council Future Fellowship (FT100100910). Thanks to the AusPlots Rangelands team (particularly Emrys Leitch,
15 Christina Pahl and Ben Sparrow) for undertaking field work and detailed consultation; Rosemary Taplin, Peter Latz and Emrys Leitch for plant identification; Belinda Medlyn for insisting that the assumptions in the LPJ model must be tested; Yusuke Onoda for providing the empirical relationship between LMA and cell-wall N. Discussions with Yan-Shih Lin and Han Wang helped to improve the data analysis. This work is a contribution to the AXA Chair Programme in Biosphere and Climate Impacts and the
20 Imperial College Initiative on Grand Challenges in Ecosystems and the Environment.



References

- Ackerly, D.D. and Cornwell, W.K.: A trait based approach to community assembly: partitioning of species trait values into within and among community components, *Ecol. Lett.*, 10, 135-145, 2007.
- 5 Ali, A. A., Xu, C., Rogers, A., McDowell, N. G., Medlyn, B. E., Fisher, R. A., Wullschlegel, S. D., Reich, P. B., Vrugt, J. A., Bauerle, W. L., Santiago, L. S., and Wilson, C. J.: Global scale environmental control of plant photosynthetic capacity, *Ecol. Appl.*, doi:10.1890/14-2111.1, 2015.
- Bernacchi, C.J., Singsaas, E.L., Pimentel, C., Portis Jr, A.P. and Long, S.P.: Improved temperature
10 response functions for models of Rubisco limited photosynthesis, *Plant Cell Environ.*, 24, 253-259, 2001.
- Bradshaw, A.D.: Evolutionary significance of phenotypic plasticity in plants, *Adv. Genet.*, 13, 115-155, 1995.
- Cernusak, L.A., Ubierna, N., Winter, K., Holtum, J.A., Marshall, J.D. and Farquhar G.D.:
15 Environmental and physiological determinants of carbon isotope discrimination in terrestrial plants, *New Phytol.*, 200, 950-965. 2003.
- Chapin III, F.S. and Kedrowski, R.A.: Seasonal changes in nitrogen and phosphorus fractions and autumn retranslocation in evergreen and deciduous taiga trees, *Ecology*, 64, 376-391, 1983.
- Chen, J.L., Reynolds, J.F., Harley, P.C. and Tenhunen, J.D.: Coordination theory of leaf nitrogen
20 distribution in a canopy, *Oecologia*, 93, 63-69, 1993.
- Dewar, R.C.: The correlation between plant growth and intercepted radiation: an interpretation in terms of optimal plant nitrogen content, *Ann. Bot.*, 78, 125-136, 1996.
- Erskine, P.D., Stewart, G.R., Schmidt, S., Turnbull, M.H., Unkovich, M. and Pate J.S.: Water
25 availability - a physiological constraint on nitrate utilization in plants of Australia semi-arid mulga woodlands, *Plant Cell Environ.*, 19, 1149-1159, 1996.
- Evans, J.R.: Photosynthesis and nitrogen relationships in leaves of C3 plants, *Oecologia*, 78, 9-19, 1989.
- Evans, J.R. and Seemann, J.R.: The allocation of protein nitrogen in the photosynthetic apparatus: costs, consequences and control, In: *In Photosynthesis*, Brigs, W.R. (Eds.), Alan R. Liss, New York, 183-205, 1989.



- Field, C. : Allocating leaf nitrogen for the maximization of carbon gain: leaf age as a control on the allocation program, *Oecologia*, 56, 34-347, 1983.
- Field, C. and Mooney, H.A.: Photosynthesis and nitrogen relationships in wild plants, In: *On the economy of plant form and function*, Givnish, T.J. (Eds.), Cambridge University Press, Cambridge, 25-55, 1986.
- 5
- Fisher, R. A., Muszala, S., Versteinstein, M., Lawrence, P., Xu, C., McDowell, N. G., Knox, R. G., Koven, C., Holm, J., Rogers, B. M., Lawrence, D., and Bonan, G.: Taking off the training wheels: the properties of a dynamic vegetation model without climate envelopes, *Geosci. Model Dev. Discuss.*, 8, 3293–3357, doi:10.5194/gmdd-8-3293-2015, 2015.
- 10
- Fyllas, N., Gloor, E., Mercado, L. M., Sitch, S., Quesada, C. A., Domingues, T. F., Galbraith, D. R., Torre-Lezama, A., Vilanova, E., Ramírez-Angulo, H., Higuchi, N., Neill, D. A., Silveira, M., Ferreira, L., Aymard, G. A., Malhi, Y., Phillips, O. L. and Lloyd, J.: Analysing Amazonian forest productivity using a new individual and trait-based model (TFS v.1), *Geosci. Model Dev.*, 7, 1251-1269, 2014.
- 15
- Gallego-Sala, A., Clark J., House J., Orr H., Prentice I.C., Smith P., Farewell, T. and Chapman, S.: Bioclimatic envelope model of climate change impacts on blanket peatland distribution in Great Britain, *Clim. Res.*, 45, 151-162, 2010.
- Guerschman, J.P., Hill, M.J., Renzullo, L.J, Barrett, D.J., Marks, A.S., Botha, E.J.: Estimating fractional cover of photosynthetic vegetation, non-photosynthetic vegetation and bare soil in the Australian tropical savanna region upscaling the EO-1 Hyperion and MODIS sensors, *Remote Sens. Environ.*, 5, 928-945, 2009.
- 20
- Gutschick, V.P.: Evolved strategies in nitrogen acquisition by plants, *American Naturalist*, 188, 607-637, 1981.
- Harrison, S.P., Prentice, I.C., Barboni, D., Kohfeld, K.E., Ni, J. and Sutra, J.P.: Ecophysiological and bioclimatic foundations for a global plant functional classification, *J. Veg. Sci.*, 21, 300-317, 2010.
- 25
- Haxeltine, A. and Prentice, I.C.: A general model for the light use efficiency of primary production, *Funct. Ecol.*, 10, 551-561, 1996.
- Hikosaka, K. and Shigeno, A.: The role of Rubisco and cell walls in the interspecific variation in photosynthetic capacity, *Oecologia*, 160, 443-451, 2009.
- 30



- Kattge, J., Knorr, W., Raddatz, T. and Wirth, C.: Quantifying photosynthetic capacity and its relationship to leaf nitrogen content for global-scale terrestrial biosphere models, *Glob. Change Biol.*, 15, 976-991, 2009.
- Kattge, J., Díaz, S., Lavorel, S., Prentice, I.C., Leadley, P. Bönisch, G., Garnier, E., Westoby, M., Reich, P.B. and Wright, I.J.: TRY – a global database of plant traits, *Glob. Change Biol.*, 17, 2905-2935, 2011.
- Lampert, D.T. and Northcote, D.: Hydroxyproline in primary cell walls of higher plants, *Nature*, 188, 665-666, 1960.
- Leigh, A., Sevanto, S., Ball, M. C., Close, J. D., Ellsworth, D. S., Knight, C. A., Nicotra, A. and Vogel, S.: Do thick leaves avoid thermal damage in critically low wind speeds? *New Phytol.*, 194, 477-487, 2012.
- Long, S. P., Postl, W. F. and Bolhar-Nordenkamp, H. R.: Quantum yields for uptake of carbon dioxide in C₃ vascular plants of contrasting habitats and taxonomic groupings, *Planta*, 189, 226-234, 1993.
- Luo, Y., Su, B., Currie, W.S., Dukes, J.S., Finzi, A., Hartwig, U., Hungate, B., McMurtrie, R.E., Oren, R. and Parton, W.J.: Progressive nitrogen limitation of ecosystem responses to rising atmospheric carbon dioxide, *Bioscience*, 54, 731-739, 2004.
- Maire, V., Martre, P., Kattge, J., Gastal, F., Esser, G., Fontaine, S. and Soussana, J.F.: The coordination of leaf photosynthesis links C and N fluxes in C₃ plant species, *PLoS ONE*, 7, e38345, doi: 10.1371/journal.pone.0038345, 2012
- Meng, T., Wang, H., Harrison, S.P., Prentice, I.C., Ni, J. and Wang, G.: Responses of leaf traits to climatic gradients: adaptive variation vs. compositional shifts, *Biogeosci.*, 12, 5339-5352, 2015.
- Niinemets, Ü. and Tenhunen, J.: A model separating leaf structural and physiological effects on carbon gain along light gradients for the shade-tolerant species *Acer saccharum*, *Plant, Cell Environ.*, 20, 845-866, 1997.
- Niinemets, Ü.: Global-scale climatic controls of leaf dry mass per area, density, and thickness in trees and shrubs, *Ecology*, 82, 453-469, 2001.
- Onoda, Y., Hikosaka K. and Hirose, T.: Allocation of nitrogen to cell walls decreases photosynthetic nitrogen-use efficiency, *Funct. Ecol.*, 18, 419-425, 2004.



- Prentice, I.C. and Cowing, S.A. Dynamic global vegetation models, In: Encyclopedia of Biodiversity, 2nd edn, Levin, S.A. (Eds.), Waltham, MA, Academic Press, 670-689, 2013.
- Prentice, I.C., Dong, N., Gleason, S.M., Maire, V. and Wright, I.J.: Balancing the costs of carbon gain and water transport: testing a new theoretical framework for plant functional ecology, *Ecol. Lett.*, 5 17, 82-91, doi: 10.1111/ele.12211, 2014.
- Prentice, I.C., Kelley, D.I., Harrison, S.P., Bartlein, P.J., Foster, P.N. and Friedlingstein, P.: Modeling fire and the terrestrial carbon balance, *Glob. Biogeochem. Cycles*, 25, GB3005, doi: 10.1029/2010GB003906, 2011a.
- Prentice, I.C., Meng, T., Wang, H., Harrison, S.P., Ni, J. and Wang, G.: Evidence of a universal scaling 10 relationship for leaf CO₂ drawdown along an aridity gradient, *New Phytol.*, 190, 169-180, 2011b.
- R Core Team: R: A language and environment for statistical computing, R Foundation for Statistical Computing, Vienna, Austria. <http://www.R-project.org/>, 2015.
- Reich, P.B., Walters, M.B. and Ellsworth, D.S.: Leaf age and season influence the relationships 15 between leaf nitrogen, leaf mass per area and photosynthesis in maple and oak trees, *Plant Cell Environ.*, 14, 251-259, 1991.
- Sakschewski, B., von Bloh, W., Boit, A., Rammig, A., Kattge, J., Poorter, L., Peñuelas, J. and Thonicke, K.: Leaf and stem economics spectra drive diversity of functional plant traits in a dynamic global vegetation model, *Glob. Change Biol.*, 21, 2711-2725, 2015.
- 20 Scheiter, S., Langan, L. and Higgins, S.I.: Next-generation dynamic global vegetation models: learning from community ecology, *New Phytol.*, 198, 957-969, doi: 10.1111/nph.12210, 2013.
- Sitch, S., Smith, B., Prentice, I.C., Arneth, A., Bondeau, A., Cramer, W., Kaplan, J.O., Levis, S., Lucht, W. and Sykes, M.T.: Evaluation of ecosystem dynamics, plant geography and terrestrial carbon cycling in the LPJ dynamic global vegetation model, *Glob. Change Biol.*, 9, 161-185, 2003.
- 25 Smith, B., Prentice, I.C. and Sykes, M.T.: Representation of vegetation dynamics in the modelling of terrestrial ecosystems: comparing two contrasting approaches within European climate space, *Glob. Ecol. Biogeogr.*, 10, 621-637, 2001.
- Stocker, B.D., Roth, R., Joos, F., Spahni, R., Steinacher, M., Zaehle, S., Bouwman, L. and Prentice, I.C.: Multiple greenhouse-gas feedbacks from the land biosphere under future climate change 30 scenarios, *Nat. Clim. Change*, 3, 666-672, doi: 10.1038/nclimate1864, 2013.



- Sultan, S.E.: Phenotypic plasticity for plant development, function and life history, *Trends Plant Sci.*, 5, 537-542, doi: 10.1016/S1360-1385 (00) 01797-0, 2000.
- Takashima, T., Hikosaka, K. and Hirose, T.: Photosynthesis or persistence: nitrogen allocation in leaves of evergreen and deciduous *Quercus* species, *Plant Cell Environ.*, 27, 1047-1054, 2004.
- 5 Thornton, P.E., Lamarque, J.F., Rosenbloom, N.A. and Mahowald, N.M.: Influence of carbon-nitrogen cycle coupling on land model response to CO₂ fertilization and climate variability, *Glob. Biogeochem. Cycles*, 21, GB4018, doi:10.1029/2006GB002868, 2007.
- Van Bodegom, P.M., Douma, J.C. and Verheijen, L.M.: A fully traits-based approach to modeling global vegetation distribution, *Proc. Natl. Acad. Sci. U.S.A.*, 111, 13733-13738, 2014.
- 10 White, A., Sparrow, B., Leitch, E., Foulkes, J., Flitton, R., Lowe, A. J. and Caddy-Retalic, S.: *AusPlots Rangelands Survey Protocols Manual, Version 1.2.9.*, University of Adelaide Press, 2012.
- Wohlfahrt, G., Bahn, M., Haubner, E., Horak, I., Michaeler, W., Rottmar, K., Tappeiner, U. and Cernusca, A.: Inter-specific variation of the biochemical limitation to photosynthesis and related leaf traits of 30 species from mountain grassland ecosystems under different land use, *Plant Cell Environ.*, 22, 1281-1296, 1999.
- 15 Wright, I.J. and Cannon, K.: Relationships between leaf lifespan and structural defences in a low-nutrient, sclerophyll flora, *Funct. Ecol.*, 15, 351-359, 2001.
- Wright, I.J. and Westoby, M.: Leaves at low versus high rainfall: coordination of structure, lifespan and physiology, *New Phytol.*, 155, 403-416, 2002.
- 20 Wright, I.J., Reich, P.B. and Westoby, M.: Least-cost input mixtures of water and nitrogen for photosynthesis, *Am. Nat.*, 161, 98-111, 2003.
- Wright, I. J., Reich, P. B., Westoby, M., Ackerly, D. D., Baruch, Z., Bongers, F., Cavender-Bares, J., Chapin, T., Cornelissen, J. H. C., Diemer, M., Flexas, J., Garnier, E., Groom, P. K., Gulias, J., Hikosaka, K., Lamont, B. B., Lee, T., Lee, W., Lusk, C., Midgley, J. J., Navas, M.-L., Niinemets, U., Oleksyn, J., Osada, N., Poorter, H., Poot, P., Prior, L., Pyankov, V. I., Roumet, C., Thomas, S. C., Tjoelker, M. G., Veneklaas, E. J., and Villar, R.: The worldwide leaf economics spectrum, *Nature*, 428, 821-827, 2004.
- 25 Wright, I.J., Reich, P.B., Cornelissen, J.H.C., Falster, D.S., Groom, P.K., Hikosaka, K., Lee, W., Lusk, C.H., Niinemets, Ü., Oleksyn, J., Osada, N., Poorter, H., Warton, D.I and Westoby, M.:



Modulation of leaf economic traits and trait relationships by climate, *Global Ecol. and Biogeogr.*, 14, 411-421, 2005.

Xu-Ri and Prentice, I.C.: Terrestrial nitrogen cycle simulation with a dynamic global vegetation model, *Glob. Chang. Biol.*, 14, 1745-1764, 2008.

- 5 Zaehle, S. and Friend, A.D.: Carbon and nitrogen cycle dynamics in the O-CN land surface model: 1. Model description, site-scale evaluation, and sensitivity to parameter estimates, *Glob. Biogeochem Cycles*, 24, GB1005, doi:10.1029/2009GB003521, 2010.



Table 1. Linear regression coefficients for $\ln N_{area}$ (g m^{-2}) as a function of $c_i:c_a$ (from $\delta^{13}\text{C}$), \ln (mean canopy PAR, I_L) ($\mu\text{mol m}^{-2} \text{s}^{-1}$), MAT ($^{\circ}\text{C}$), \ln LMA (g m^{-2}) and the factor ‘N-fixer’ at species level.

| | Estimated | Predicted | p | R^2 |
|-----------|--------------------|-----------|----------|-------|
| $c_i:c_a$ | -0.611 ± 0.252 | -0.615 | <0.01 | 55% |
| $\ln I_L$ | 0.874 ± 0.096 | 1 | <0.001 | |
| MAT | -0.047 ± 0.007 | -0.048 | <0.001 | |
| \ln LMA | 0.415 ± 0.036 | n/a | <0.001 | |
| ‘N-fixer’ | 0.306 ± 0.041 | n/a | <0.001 | |



Table 2. Linear regression coefficients for community-mean (simple average) values of $\ln N_{area}$ (g m^{-2}) as a function of $c_i:c_a$ (from $\delta^{13}\text{C}$), \ln (mean canopy PAR, I_L) ($\mu\text{mol m}^{-2} \text{s}^{-1}$), MAT ($^{\circ}\text{C}$) and \ln LMA (g m^{-2}).

| | Estimated | Predicted | p | R^2 |
|-----------|--------------------|-----------|----------|-------|
| $c_i:c_a$ | -1.60 ± 0.94 | -0.615 | n.s. | 82% |
| $\ln I_L$ | 0.70 ± 0.23 | 1 | <0.001 | |
| MAT | -0.035 ± 0.016 | -0.048 | <0.001 | |
| \ln LMA | 0.57 ± 0.19 | n/a | <0.001 | |

5



Table 3. Linear regression coefficients for N_{area} as a function of independently predicted values of $N_{rubisco}$ and $N_{structure}$ (all in g m^{-2}) at species level.

| | Estimated | Predicted | P | R^2 |
|-----------------------------|---------------|-----------|--------|-------|
| $N_{rubisco}$ | 9.5 ± 2.0 | 6-20 | <0.001 | 52% |
| $N_{structure}$ | 1.2 ± 0.2 | 1 | <0.001 | |
| $N_{structure}$: 'N-fixer' | 1.0 ± 0.3 | n/a | <0.01 | |



Figures.

Fig 1 Site locations, climate and leaf trait distributions: Mean annual precipitation (MAP, mm), mean annual temperature (MAT, °C), mean incident daytime photosynthetically active radiation (PAR, $\mu\text{mol m}^{-2} \text{s}^{-1}$), moisture index (MI). Site mean N_{area} (g m^{-2}) and LMA (g m^{-2}) are also shown.

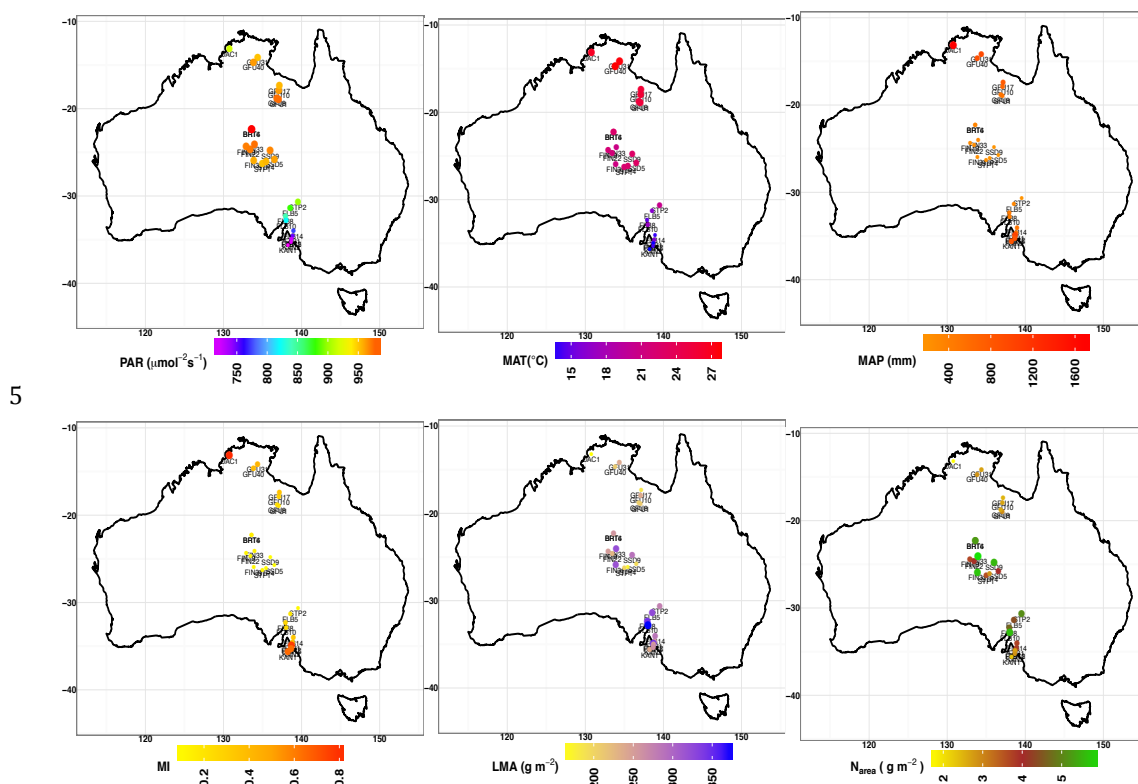
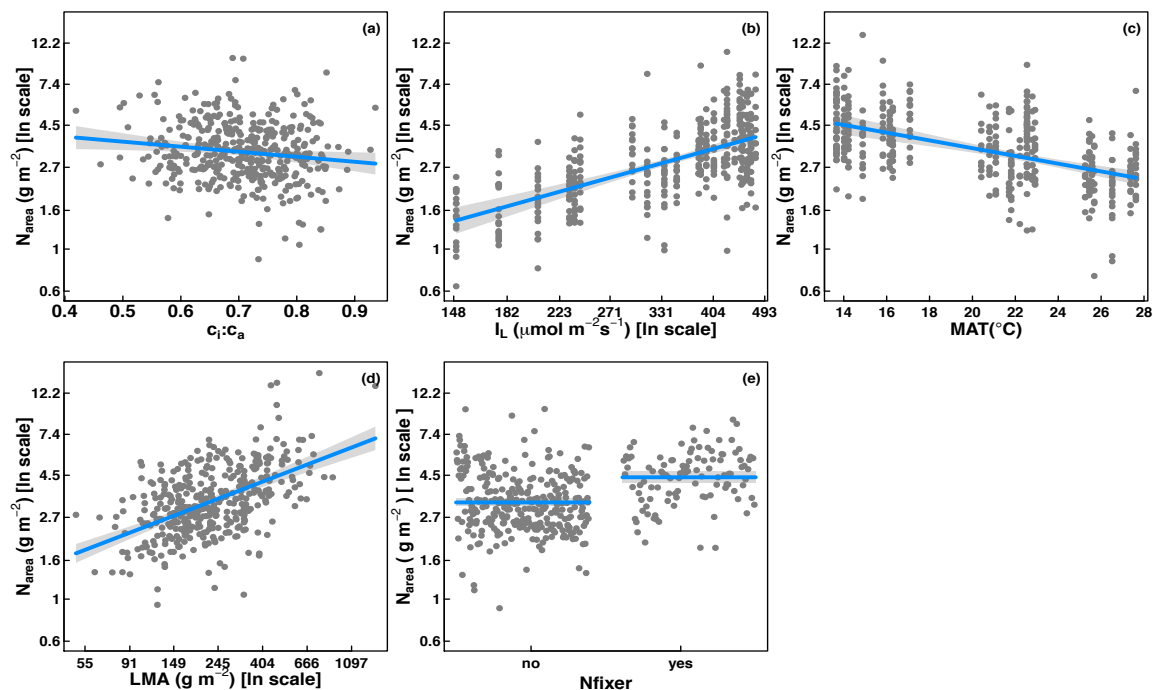




Fig 2. Partial residual plots for the regression of $\ln N_{area}$ (g m^{-2}) as a function of $c_i:c_a$ (from $\delta^{13}\text{C}$), \ln (mean canopy PAR, I_L) ($\mu\text{mol m}^{-2} \text{s}^{-1}$), MAT ($^{\circ}\text{C}$), \ln LMA (g m^{-2}) and the factor ‘N-fixer’ at species level. Note the logarithmic scale of the y-axis.



5



Fig 3. Partial residual plots for the linear regression of N_{area} as a function of independently predicted values of $N_{rubisco}$ and $N_{structure}$ (all in g m^{-2}) at species level. Blue: N-fixers, red: non-N-fixers.

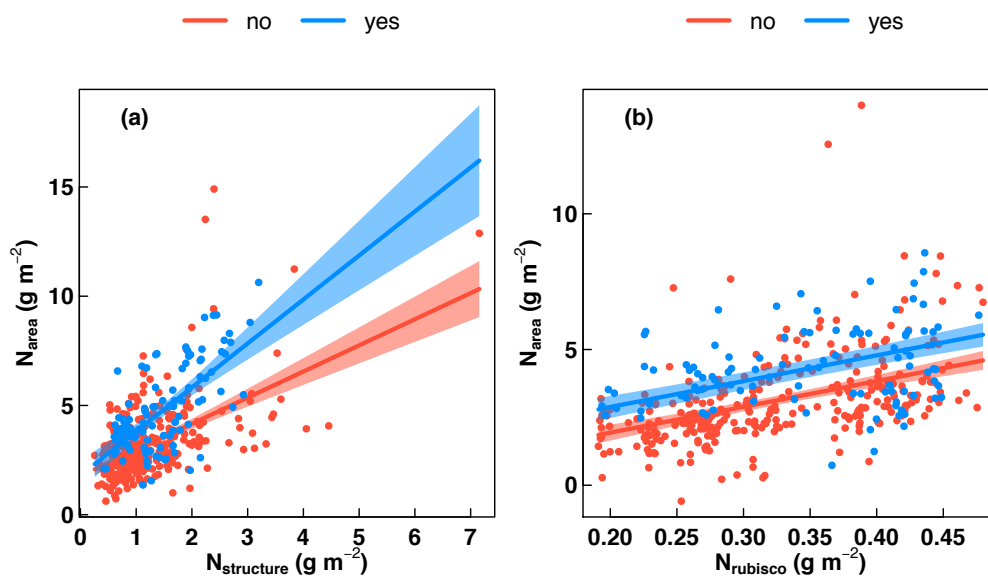




Fig 4. Trait means and regression lines for all 243 C_3 plant species in the 27 study sites. Note the logarithmic scales for N_{area} (g m^{-2}) and LMA (g m^{-2}). Thin red dashed lines represent individual within-species regression lines of non-N-fixer species. Thin blue lines represent individual within-species regression lines of N-fixer species. The black dashed line represents the overall regression line, which has a slope of unity by definition. Grey dots denote individual species-site combinations. Common within-species slopes are 0.53 ± 0.11 ($\ln N_{area}$), 1.02 ± 0.12 ($c_i:c_a$) and 0.55 ± 0.11 ($\ln \text{LMA}$)

